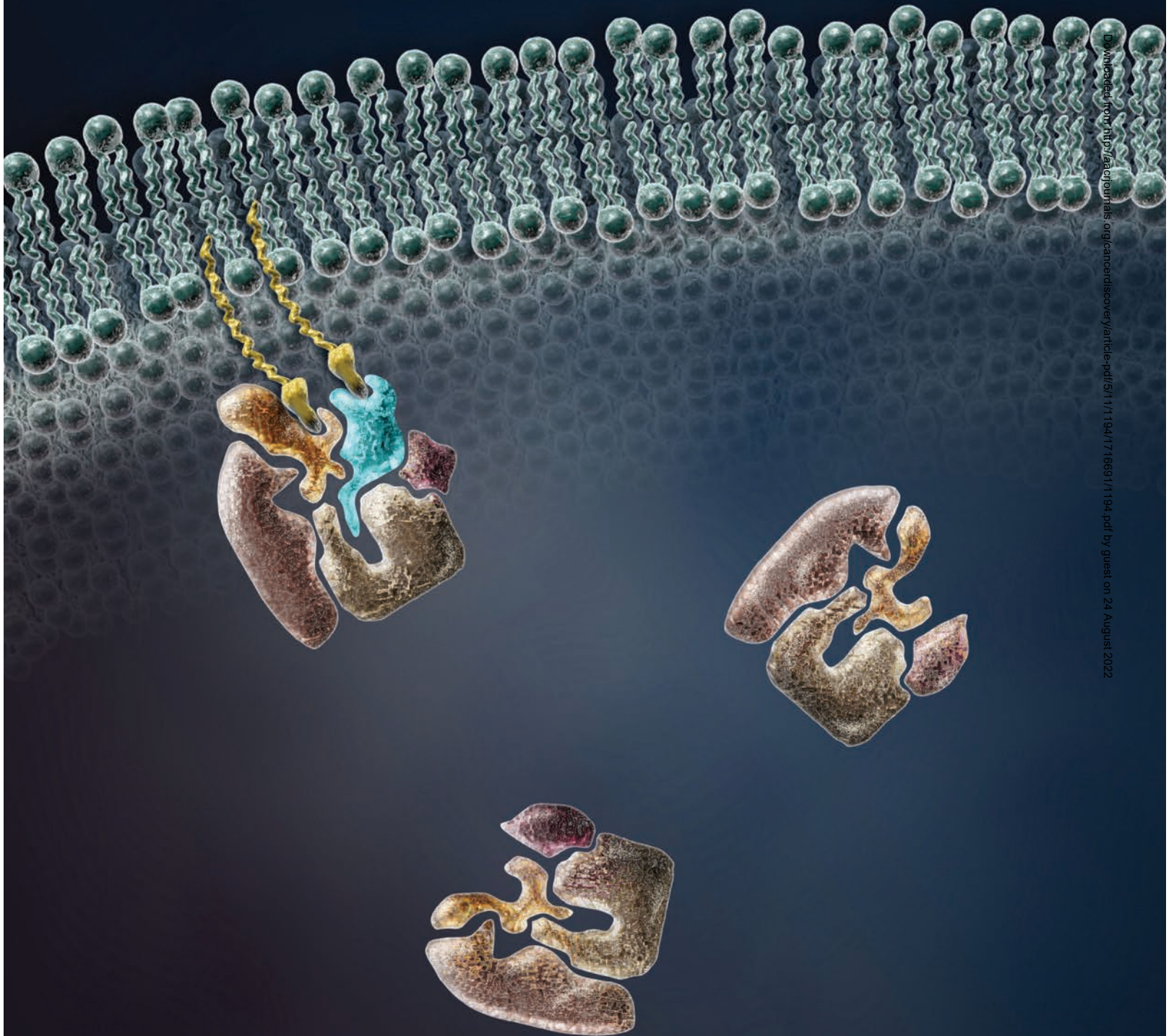


PtdIns(3,4,5)P₃-Dependent Activation of the mTORC2 Kinase Complex

Pengda Liu¹, Wenjian Gan¹, Y. Rebecca Chin¹, Kohei Ogura¹, Jianping Guo¹, Jinfang Zhang¹, Bin Wang¹, John Blenis², Lewis C. Cantley², Alex Toker¹, Bing Su^{3,4}, and Wenyi Wei¹



ABSTRACT

mTOR serves as a central regulator of cell growth and metabolism by forming two distinct complexes, mTORC1 and mTORC2. Although mechanisms of mTORC1 activation by growth factors and amino acids have been extensively studied, the upstream regulatory mechanisms leading to mTORC2 activation remain largely elusive. Here, we report that the pleckstrin homology (PH) domain of SIN1, an essential and unique component of mTORC2, interacts with the mTOR kinase domain to suppress mTOR activity. More importantly, PtdIns(3,4,5) P_3 , but not other PtdIns P_n species, interacts with SIN1-PH to release its inhibition on the mTOR kinase domain, thereby triggering mTORC2 activation. Mutating critical SIN1 residues that mediate PtdIns(3,4,5) P_3 interaction inactivates mTORC2, whereas mTORC2 activity is pathologically increased by patient-derived mutations in the SIN1-PH domain, promoting cell growth and tumor formation. Together, our study unravels a PI3K-dependent mechanism for mTORC2 activation, allowing mTORC2 to activate AKT in a manner that is regulated temporally and spatially by PtdIns(3,4,5) P_3 .

SIGNIFICANCE: The SIN1-PH domain interacts with the mTOR kinase domain to suppress mTOR activity, and PtdIns(3,4,5) P_3 binds the SIN1-PH domain to release its inhibition on the mTOR kinase domain, leading to mTORC2 activation. Cancer patient-derived SIN1-PH domain mutations gain oncogenicity by loss of suppressing mTOR activity as a means to facilitate tumorigenesis. *Cancer Discov*; 5(11); 1194–209. ©2015 AACR.

See related commentary by Yuan and Guan, p. 1127.

INTRODUCTION

mTOR is an evolutionarily conserved Ser/Thr kinase essential for pivotal cellular and physiologic functions, including cell growth, proliferation, and metabolism (1). Hyperactivation of mTOR signaling is observed in virtually all human solid tumors and hematologic malignancies, as well as diabetes and neurodegeneration (1). Structurally, mTOR serves as an indispensable catalytic subunit for two functionally distinct subcomplexes termed mTOR complex 1 (mTORC1) and mTOR complex 2 (mTORC2). Both mTORC1 and mTORC2 share two common subunits, mTOR and GβL, whereas RPTOR is a unique component of mTORC1 (2), and both RICTOR (3) and SIN1 (4–6) are restricted to mTORC2.

Importantly, both mTORC1 and mTORC2 sense cellular physiologic cues, but with different specificities to ensure that cells proliferate only under favorable conditions. Specifically,

activation of mTORC1 requires at least two types of stimulation. Triggered by amino acids or nutrients, mTORC1 is recruited to the surface of lysosomes in an amino-acid transporter SLC38A9 (7, 8), Rag-GTPase (9), Ragulator (10), and vacuolar adenosine triphosphatase (11)–dependent manner through an “inside-out” mechanism (12). However, full activation of mTORC1 also requires a lysosomal, GTP-loaded active form of RHEB, resulting from the release of TSC2 inhibitory effects on RHEB through phosphorylation of TSC2 by various growth signaling pathways, including PI3K/AKT signaling (13), RAS/ERK signaling (14), or WNT signaling (15). Interestingly, amino-acid-specific activation mechanisms were also identified, where leucine relies on the RAG-GTPase, whereas glutamine depends on the adenosine-diphosphate-ribosylation-factor-1 GTPase instead of RAG for mTORC1 lysosome translocation and activation (16).

In contrast, mTORC2 is primarily activated by extracellular stimuli, such as growth factors and insulin (17, 18). However, the detailed molecular mechanisms leading to mTORC2 activation have just begun to be explored. To this end, mTORC2 activation has been reported to require ribosome association (19) and to facilitate cotranslational phosphorylation of AKT on Thr450 for stabilization of newly synthesized AKT protein (20). Furthermore, mTORC2 has been reported to locate proximal to endoplasmic reticulum (ER), mitochondria, mitochondria-associated ER-membrane (MAM), or the nucleus in different mammalian cells and near the plasma membrane (PM) in yeast (17). However, how growth factor signaling, which initiates from extracellular signals and occurs primarily at the PM, governs mTORC2 activation to subsequently activate AKT, is poorly understood.

Here, we report that mTORC2 is activated through a “release-of-inhibition” mechanism by growth signaling molecules in a PtdIns(3,4,5) P_3 -dependent manner occurring at the PM proximity, which reveals a critical molecular mechanism underlying how aberrant alternation of the PtdIns(3,4,5) P_3 -SIN1

¹Department of Pathology, Beth Israel Deaconess Medical Center, Harvard Medical School, Boston, Massachusetts. ²Cancer Center at Weill Cornell Medical College and New York-Presbyterian Hospital, New York, New York. ³Shanghai Institute of Immunology, Department of Microbiology and Immunology, Shanghai Jiao Tong University School of Medicine, Shanghai, China. ⁴Department of Immunobiology and the Vascular Biology and Therapeutics Program, Yale University, New Haven, Connecticut.

Note: Supplementary data for this article are available at Cancer Discovery Online (<http://cancerdiscovery.aacrjournals.org/>).

Corresponding Authors: Wenyi Wei, Beth Israel Deaconess Medical Center, Harvard Medical School, 330 Brookline Avenue, Boston, MA 02215. Phone: 617-735-2495; Fax: 617-735-2480; E-mail: wwei2@bidmc.harvard.edu; and Bing Su, Shanghai Institute of Immunology, Department of Microbiology and Immunology, Shanghai Jiao Tong University School of Medicine, Shanghai 200025, China, or Department of Immunobiology and the Vascular Biology and Therapeutics Program, Yale University, 333 Cedar Street, New Haven, CT 06520. Phone: 203-737-2463; E-mail: bing.su@yale.edu

doi: 10.1158/2159-8290.CD-15-0460

©2015 American Association for Cancer Research.

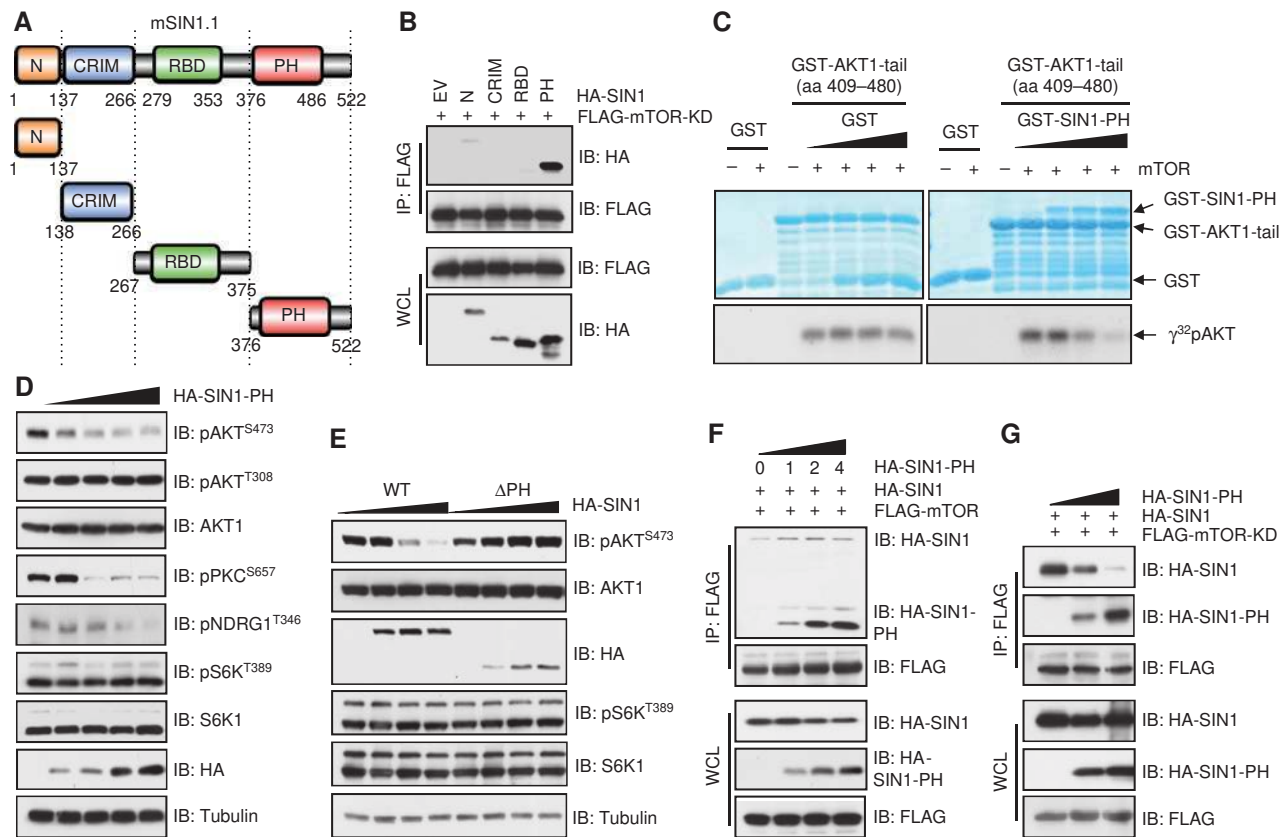


Figure 1. The PH domain of SIN1 binds the mTOR kinase domain and inhibits mTORC2 catalytic activity. **A**, a schematic illustration of the SIN1 domain structures. **B**, the SIN1-PH domain binds the mTOR kinase domain (KD; aa 2180–2431). FLAG-mTOR-KD was transfected into HEK293 cells and affinity purified by FLAG-M2 beads 48 hours after transfection. Then FLAG-mTOR-KD IPs were used to pull down indicated SIN1 truncations expressed in HEK293 cells after serum starvation for 24 hours and subjected to immunoblot (IB) analyses. **C**, SIN1-PH suppresses mTOR to phosphorylate AKT *in vitro*. *In vitro* kinase assays of recombinant active mTOR kinases with GST-AKT1-tail (aa 409–480) as a substrate, in the presence of increasing doses of bacterially purified GST or GST-SIN1-PH proteins. **D**, SIN1-PH suppresses mTORC2 activity in cells. IB of whole cell lysates (WCL) derived from MDA-MB-231 cells transfected with increasing amounts of HA-SIN1-PH. **E**, expression of full-length, but not PH domain-deleted SIN1, leads to reduced pAKT^{S473} in cells. IB analysis of WCLs derived from HEK293T cells transfected with increasing doses of HA-SIN1. **F**, binding of SIN1-PH to mTOR-KD does not disrupt mTORC2 complex integrity. IB of FLAG-IP and WCLs derived from HEK293T cells transfected with HA-SIN1, FLAG-mTOR, and increasing doses of HA-SIN1-PH. **G**, SIN1-PH competes with full-length SIN1 for binding mTOR-KD. IB analysis of WCLs and FLAG-IPs derived from HEK293T cells transfected with indicated constructs.

pleckstrin homology (PH)–mTOR signaling pathway may contribute to pathologic disorders.

RESULTS

The PH Domain of SIN1 Interacts with the mTOR Kinase Domain and Inhibits mTOR Catalytic Activity toward Phosphorylating AKT

Notably, the recently reported partial mTOR/GβL crystal structure (21) suggests an “active-site restriction” model for mTOR activity control (22), where the mTOR active site is relatively accessible, but the ability of mTOR substrates to enter the mTOR kinase active site is in part governed by mTOR-associated proteins, such as RPTOR (22). Inspired by this hypothesis, we evaluated whether the two mTORC2-specific subunits, RICTOR and SIN1, can function as possible mTOR kinase activity regulators. Interestingly, aside from the reported GβL interaction with the LBE motif (21) of the mTOR kinase domain (Supplementary Fig. S1A and S1B), we

found that only SIN1, but not RICTOR, interacted with the catalytic C-loop of the mTOR kinase domain (amino acids 2298–2518) that in large part exerts mTOR kinase activity (23) in cells (Supplementary Fig. S1C). These results indicate SIN1 as a possible modulator of mTORC2 kinase activity. Consistently, although SIN1 is essential for mTORC2 complex integrity and kinase activity (4–6), it was previously identified as an endogenous inhibitor for various stress-induced signaling components by binding directly to their catalytic domains, including MEKK2 (24), JNK (25), and RAS (ref. 26; Supplementary Fig. S1D). Notably, SIN1 binds the mTOR kinase domain (mTOR-KD; aa 2186–2431) primarily through its carboxyl-terminal PH domain and, to a much lesser extent, its N-terminus (Fig. 1A and B). Importantly, SIN1-PH, but not SIN1-N, inhibited mTOR’s ability to phosphorylate AKT^{S473} *in vitro* (Fig. 1C and Supplementary Fig. S1E) and in cells (Fig. 1D and Supplementary Fig. S1F–S1J), demonstrating the importance of the SIN1-PH domain in suppressing mTOR kinase activity. Surprisingly, expression of full-length

or N-deleted SIN1, but not PH-deleted SIN1, led to reduced AKT^{S473} phosphorylation in a SIN1 dose-dependent manner (Fig. 1E and Supplementary Fig. S1K–S1O), further supporting a negative role of the SIN1-PH domain in regulating mTORC2 activity. Therefore, in the remainder of the study, we focused on examining mechanistically how SIN1-PH may function to suppress mTORC2 activation, although we cannot exclude the possibility that the SIN1-N may also play a role in mTORC2 regulation.

To gain further insights into how SIN1-PH mediates suppression of mTOR activity, we next examined the specific region(s) of mTOR that interact(s) with SIN1-PH. Consistent with previous reports that SIN1 prefers binding enzymatic domains (24), we observed that SIN1-PH mainly bound the kinase domain of mTOR (Supplementary Fig. S1P). Moreover, SIN1-PH interacted with the large portion of the mTOR kinase domain (N-FATC, aa 2115–2549), but not the FRB region located in the N-terminus of the mTOR kinase domain (aa 2001–2114; Supplementary Fig. S1A and S1Q). Furthermore, the mTOR catalytic C-loop, but not the GβL-interacting LBE domain (ref. 22; Supplementary Fig. S1A), was necessary for mediating the SIN1-PH interaction with mTOR kinase domain (Supplementary Fig. S1R and S1S), and this interaction was recently confirmed by cross-linking experiments (27). Notably, both PFAM and Phosphosite Plus algorithms, as well as structural homology-based modeling of mTOR binding to the PIKK superfamily members (23), indicate a conserved kinase domain present in mTOR (termed KD; aa 2186–2431), which displays similar affinity as KD-L (aa 2115–2518) in associating with the SIN1-PH domain in cells (Supplementary Fig. S1T). Therefore, to possibly bypass the conformational constraints caused by utilizing only the C-loop of the mTOR kinase domain, we mainly used the mTOR-KD (Supplementary Fig. S1A) in subsequent experiments. Consistent with a critical role of SIN1-PH in suppressing mTOR-KD, deletion of the PH domain compromised SIN1 interaction with mTOR-KD (Supplementary Fig. S1U), but not full-length mTOR (Supplementary Fig. S1V), possibly through an mTOR-independent manner, as SIN1 could bind multiple mTORC2 components including RICTOR and GβL other than mTOR itself (28, 29). Notably, expression of SIN1-PH did not interfere with the mTORC2 complex integrity (Fig. 1F and Supplementary Fig. S1W–S1X), but competed with full-length SIN1 for mTOR-KD interaction (Fig. 1G). Together, these data demonstrate that SIN1-PH interacts with mTOR-KD to suppress mTOR kinase activity (Supplementary Fig. S1Y).

The SIN1-PH Motif Is a Physiologic PH Domain That Can Functionally Replace the AKT1-PH Domain in Cells

The PH domain is characterized by its affinity and specificity for binding phosphatidylinositol phosphates (PtdInsP_n) with at least one pair of adjacent phosphates within the inositol headgroups (30). However, only ~10% of all PH domains display PtdInsP_n-binding specificity and affinity (30). In support of a unique feature for SIN1-PH in suppressing mTOR kinase activity, expression of either the AKT1-PH domain (Supplementary Fig. S2A) or the PDK1-PH domain (Supplementary Fig. S2A and S2B) did not significantly affect

AKT^{S473} phosphorylation in cells. To gain further insights into the physiologic role of SIN1-PH in cells, we found that deletion of the AKT1-PH domain significantly abrogated AKT phosphorylation (Fig. 2A and B), whereas substitution of AKT1-PH with SIN1-PH (Fig. 2A) could largely functionally reconstitute phosphorylation of AKT^{S473} but not AKT^{T308} in cells (Fig. 2B) upon stimulation (Fig. 2C and D and Supplementary Fig. S2C), suggesting a potential physiologic PtdInsP_n-binding function for the SIN1-PH domain.

PtdIns(3,4,5)P₃ Specifically Interacts with the SIN1-PH Domain to Promote AKT Activation at the PM

To examine the phosphoinositide-binding specificity of the SIN1-PH domain, we first used PtdInsP_n overlay assays to map that SIN1-PH bound preferentially *in vitro* to PtdIns(3,4,5)P₃ and PtdIns(3,5)P₂, and to a lesser extent, PtdIns5P and PA (Fig. 3A). However, as all PtdInsP_ns are immobilized in these overlay assays, these experiments may not faithfully mimic physiologic conditions. Therefore, we further examined the specificity of agarose-beads-coupled “PIPsomes” that better mimic physiologic PtdInsP_n species in interacting with SIN1. Importantly, under this relatively more physiologic condition, only PIPsomes containing PtdIns(3,4,5)P₃, but not those with PtdIns(3,5)P₂, were able to pull down SIN1 (Fig. 3B). Notably, other mTORC2 components were not pulled down in the triton buffer used, which disrupts the integrity of the mTORC2 complex (31). Furthermore, SIN1 mainly interacted with PtdIns(3,4,5)P₃, but not other PtdInsP_n species examined (Fig. 3C), highlighting that, like AKT-PH (32), SIN1-PH is largely a PtdIns(3,4,5)P₃-binding motif. In keeping with PtdIns(3,4,5)P₃ as a critical upstream mediator for mTORC2 function, inhibition of pan-PI3K (using wortmannin, LY2940002, and PLK90) or p110α and p110β (using BKM120), both of which produce PtdIns(3,4,5)P₃, but not PIKFYVE (by YM201636) that produces PtdIns(3,5)P₂ (33), led to reduced AKT phosphorylation in cells (Fig. 3D and Supplementary Fig. S3A and S3B). Consistently, depletion of p110α (PIK3CA; Fig. 3E and F and Supplementary Fig. S3C), but not PIKFYVE (Fig. 3G and H and Supplementary Fig. S3D), resulted in reduced AKT^{S473} phosphorylation. Taken together, these data demonstrate that PtdIns(3,4,5)P₃, but not PtdIns(3,5)P₂, is the major physiologic PtdInsP_n species that governs mTORC2 activation in cells.

In agreement with the notion that the SIN1-PH domain interacts with PtdIns(3,4,5)P₃, we observed that PtdIns(3,4,5)P₃ primarily interacted with the PH motif, but not other domains of SIN1 in cells (Fig. 3I). Moreover, the SIN1-PH domain bound Ins(1,3,4,5)P₄ (the soluble headgroup of PtdIns(3,4,5)P₃; ref. 32) with a K_d comparable with that of AKT1-PH *in vitro* (Supplementary Fig. S3E and S3F). Consistently, in CHAPS buffers that retain mTORC2 integrity, PtdIns(3,4,5)P₃ beads were able to pull down intact mTORC2 complexes (Fig. 3J), in a manner that is largely mediated by SIN1, as genetic ablation of *Sin1* led to compromised RICTOR interaction with PtdIns(3,4,5)P₃ beads (Supplementary Fig. S3G). More importantly, the mTORC2 complexes isolated by PtdIns(3,4,5)P₃ pull-downs were able to phosphorylate AKT^{S473} *in vitro* (Supplementary Fig. S3H), and this phosphorylation could be antagonized by

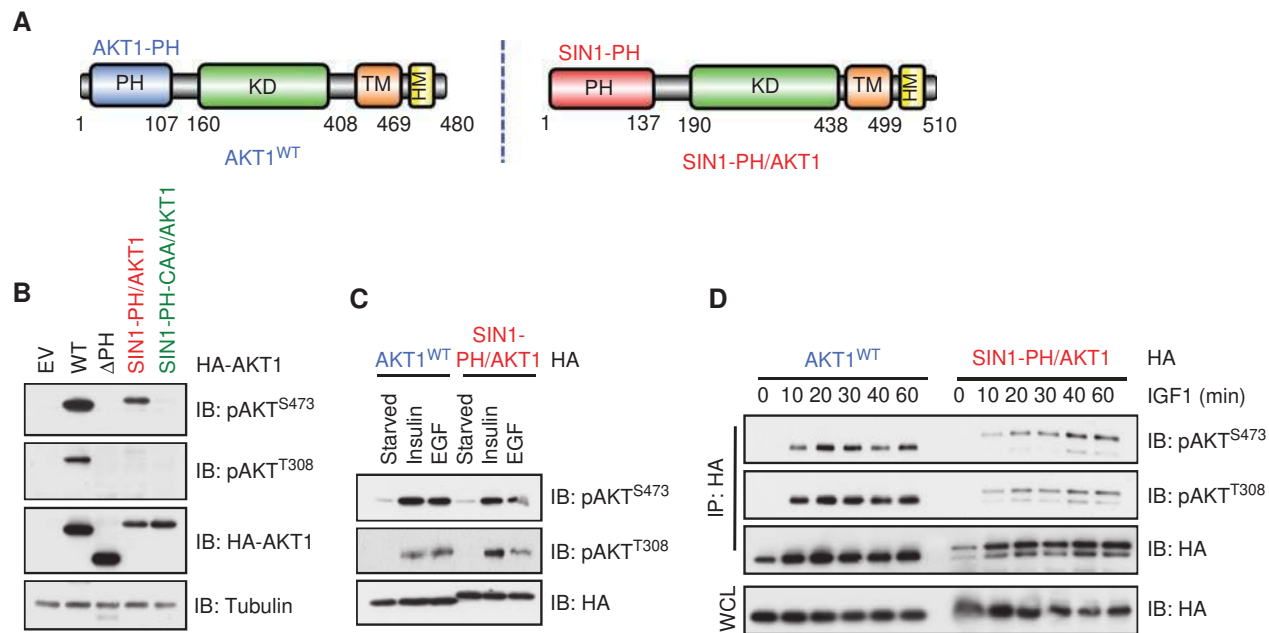


Figure 2. The PH domain of SIN1 largely replaces the PH domain of AKT1 for function in cells. **A**, a schematic illustration of the AKT1^{WT} (left) and the SIN1-PH-AKT1 chimera domain structures (right). **B**, deleting the PH domain of AKT1 leads to attenuated AKT phosphorylation. Immunoblot (IB) analysis of whole cell lysates (WCL) derived from DLD1-AKT1/2^{-/-} cells transfected with indicated constructs. **C** and **D**, SIN1-PH largely functionally replaces AKT1-PH in cells. IB of WCLs derived from AKT1/2^{-/-} mouse embryonic fibroblasts (**C**) or HeLa cells (**D**) transfected with indicated constructs. Where indicated, cells were serum starved for 12 hours before adding insulin (100 nmol/L) for 30 minutes or EGF (100 ng/mL) for 10 minutes (**C**) or IGF1 (100 ng/mL) for the indicated time periods (**D**).

pharmacologic inhibition of mTOR kinase (Supplementary Fig. S3I), suggesting that PtdIns(3,4,5)P₃-associated mTORC2 complexes are catalytically active.

Given that the mTORC2 substrate AKT is activated primarily on the PM, and mTORC2 has also been observed localized on PM in both mammalian cells (34) and yeast (35, 36), we next examined whether mTORC2 is activated on PM, such that its activation may subsequently trigger phosphorylation of PM-associated AKT on Ser473. To this end, we observed that although dispersed under serum-deprived conditions, the SIN1-PH domain accumulated proximal to the PM upon insulin stimulation (Fig. 3K). Furthermore, this localization could be blocked by pretreatment with the PI3K inhibitor PLK90 or the PIK3CA inhibitor BKM120 but not the PIK-FYVE inhibitor YM201636 (Fig. 3K). These results suggest that the SIN1-PH domain may be recruited to PM at regions with PtdIns(3,4,5)P₃, but not PtdIns(3,5)P₂ synthesis. Consistently, depletion of endogenous p110 α , but not PIK-FYVE, resulted in impaired PM localization of SIN1-PH induced by insulin (Supplementary Fig. S3J). Moreover, endogenous RICTOR was slightly enriched on PM upon insulin stimulation in *Sin1*^{+/+} but not *Sin1*^{-/-} mouse embryonic fibroblasts (MEF; Supplementary Fig. S3K–S3L), highlighting a critical role for SIN1 in the PM localization of the mTORC2 complex for its kinase activation.

PtdIns(3,4,5)P₃ Interacts with the PH Domain of SIN1 via Three Critical Residues Including R393, K428, and K464

To gain further mechanistic insights into PtdIns(3,4,5)P₃-mediated activation of mTORC2, we performed *in vitro* kinase

assays in a cell-free system. Under these conditions, consistent with a previous report (37), PtdIns(3,4,5)P₃, but not other PtdInsP_n-containing poly-PIPsomes, was able to directly trigger activation of inactive mTORC2 complexes immunoprecipitated from serum-starved cells, as measured by AKT^{S473} phosphorylation *in vitro* (Fig. 4A and B). Previous studies on PtdInsP_n-dependent activation of AKT (32) inspired us to postulate that, similar to PtdIns(3,4,5)P₃-mediated AKT activation, PtdIns(3,4,5)P₃ may also activate mTORC2 by releasing SIN1-PH inhibition on mTOR-KD. Consistently, the SIN1-PH domain interaction and suppression of the mTOR catalytic domain could be released in response to physiologic stimuli that trigger mTORC2 activity to phosphorylate AKT at S473, such as insulin (Fig. 4C) or EGF (Supplementary Fig. S4A), or by accumulated PIP₃ species through *PTEN* loss (Supplementary Fig. S4B).

We therefore examined the critical residues in the SIN1-PH domain that mediate its interaction with PtdIns(3,4,5)P₃. By comparing the AKT1-PH/Ins(1,3,4,5)P₄ crystal structure (PDB: 1H10) with a computer-modeled SIN1-PH/Ins(1,3,4,5)P₄ structure through superimposing Ins(1,3,4,5)P₄ into a characterized SIN1-PH domain structure (ref. 38; Fig. 4D and E), we identified several potential critical residues, including R393, K428, and K464, within the SIN1-PH domain that might mediate Ins(1,3,4,5)P₄ binding. The triple R393C/K428A/K464A mutant (termed CAA), but not any of the single mutants alone, was impaired in promoting AKT^{S473} phosphorylation in cells in response to IGF1 (Fig. 5A) or insulin (Supplementary Fig. S5A) in a time- (Fig. 5B) and dose-dependent (Supplementary Fig. S5B) manner. Notably, this deficiency was not due to disrupted mTORC2 integrity

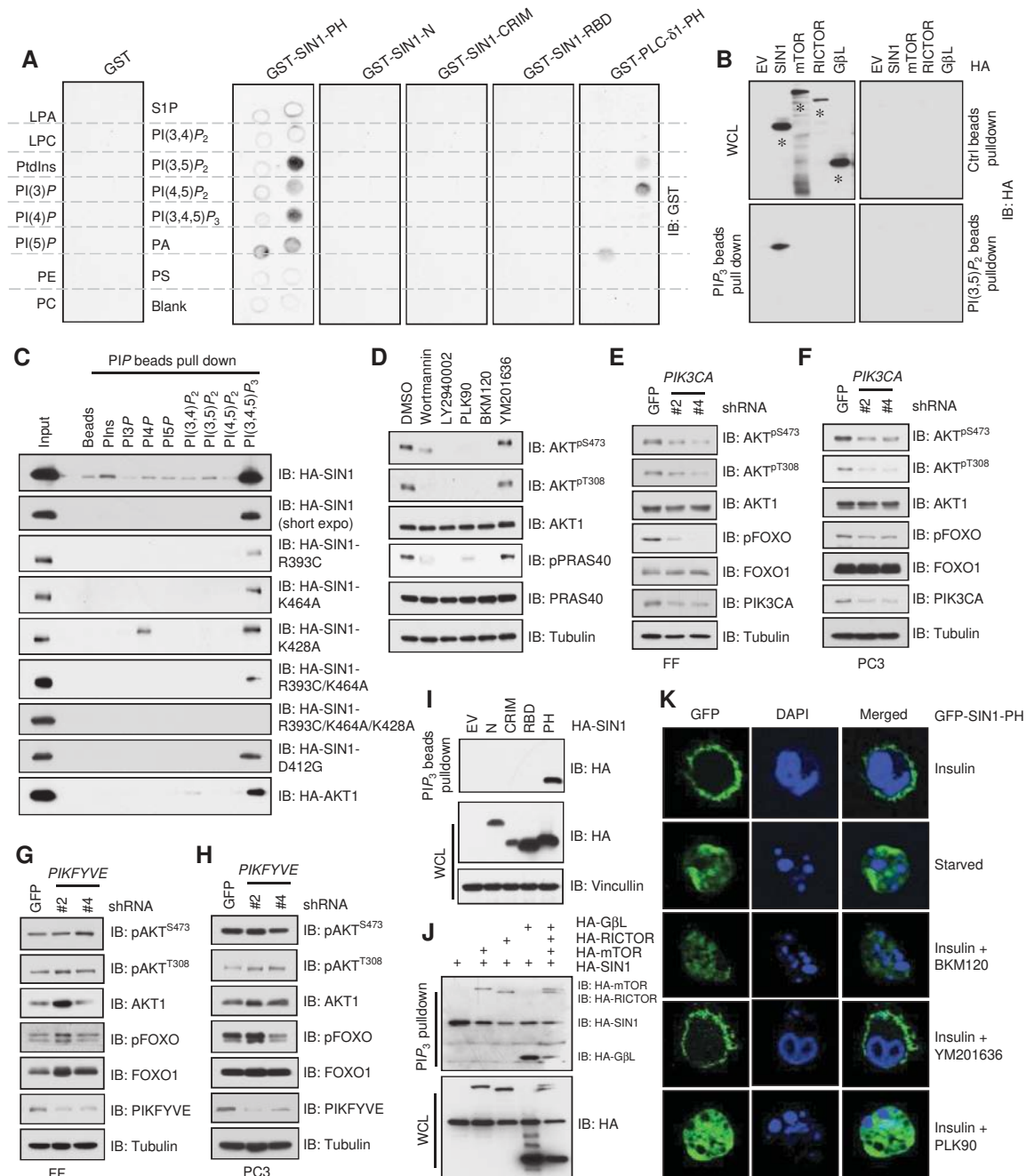


Figure 3. PI(3,4,5)P₃ directly interacts with the SIN1-PH domain and recruits mTORC2 to PM proximity. **A**, PIP₂ overlay assays indicate that GST-SIN1-PH mainly interacts with PI(3,5)P₂ and PI(3,4,5)P₃ under two-dimensional conditions. **B**, PI(3,4,5)P₃, but not PI(3,5)P₂-coupled beads pull down ectopically expressed SIN1, but not other mTORC2 components in cells. Immunoblot (IB) of indicated PIP beads pull-downs and whole cell lysates (WCL) derived from HEK293T cells transfected with indicated constructs. Asterisks indicate the positions for the labeled proteins. **C**, PI(3,4,5)P₃, but not other PIPs examined, pulled down ectopically expressed SIN1. IB of WCLs and PIP beads pull-downs derived from HEK293T cells transfected with indicated constructs. Please note that various SIN1 mutants were included here to screen for critical residues mediating the PI(3,4,5)P₃ interaction with SIN1-PH. The detailed description of these mutants can be found in Fig. 4E and Fig. 5 or associated text. **D**, inhibition of PI(3,4,5)P₃, but not PI(3,5)P₂, generation leads to reduced AKT^{S473} phosphorylation in cells. IB of WCLs derived from HeLa cells treated with indicated inhibitors for 2 hours. Drug doses used: wortmannin (100 nmol/L), LY2940002 (1 μmol/L), PLK90 (20 nmol/L), BKM120 (100 nmol/L), and YM201636 (500 nmol/L). **E–H**, depletion of endogenous PIK3CA, but not PIKFYVE, leads to attenuated mTORC2 activity toward phosphorylating AKT^{S473} in cells. IB of WCLs derived from primary foreskin fibroblasts (**E** and **G**) or PC3 (**F** and **H**) cells infected with shPIK3CA (**E** and **F**) or shPIKFYVE (**G** and **H**) lentiviruses. Seventy-two hours after puromycin selection (1 μg/mL), cells were harvested for IB analysis. **I**, PI(3,4,5)P₃ mainly binds the PH domain of SIN1. IB of PIP₃ beads pull-downs and WCLs derived from HEK293T cells transfected with indicated constructs. **J**, PI(3,4,5)P₃ pulls down intact mTORC2 complexes. IB of PIP₃ pull-downs (in CHAPS buffers) and WCLs derived from HEK293T cells transfected with indicated constructs. **K**, representative confocal images to illustrate that GFP-SIN1-PH enriches in PM proximity upon insulin (100 nmol/L) stimulation for 15 minutes, which was abolished by inhibiting PIP₃ generation via 20 nmol/L PLK90 or 100 nmol/L BKM120, but not by inhibiting PI(3,5)P₂ generation with 500 nmol/L YM201636.

Downloaded from <http://aacrjournals.org/cancerdiscovery/article-pdf/5/11/1194/1716891/1194.pdf> by guest on 24 August 2022

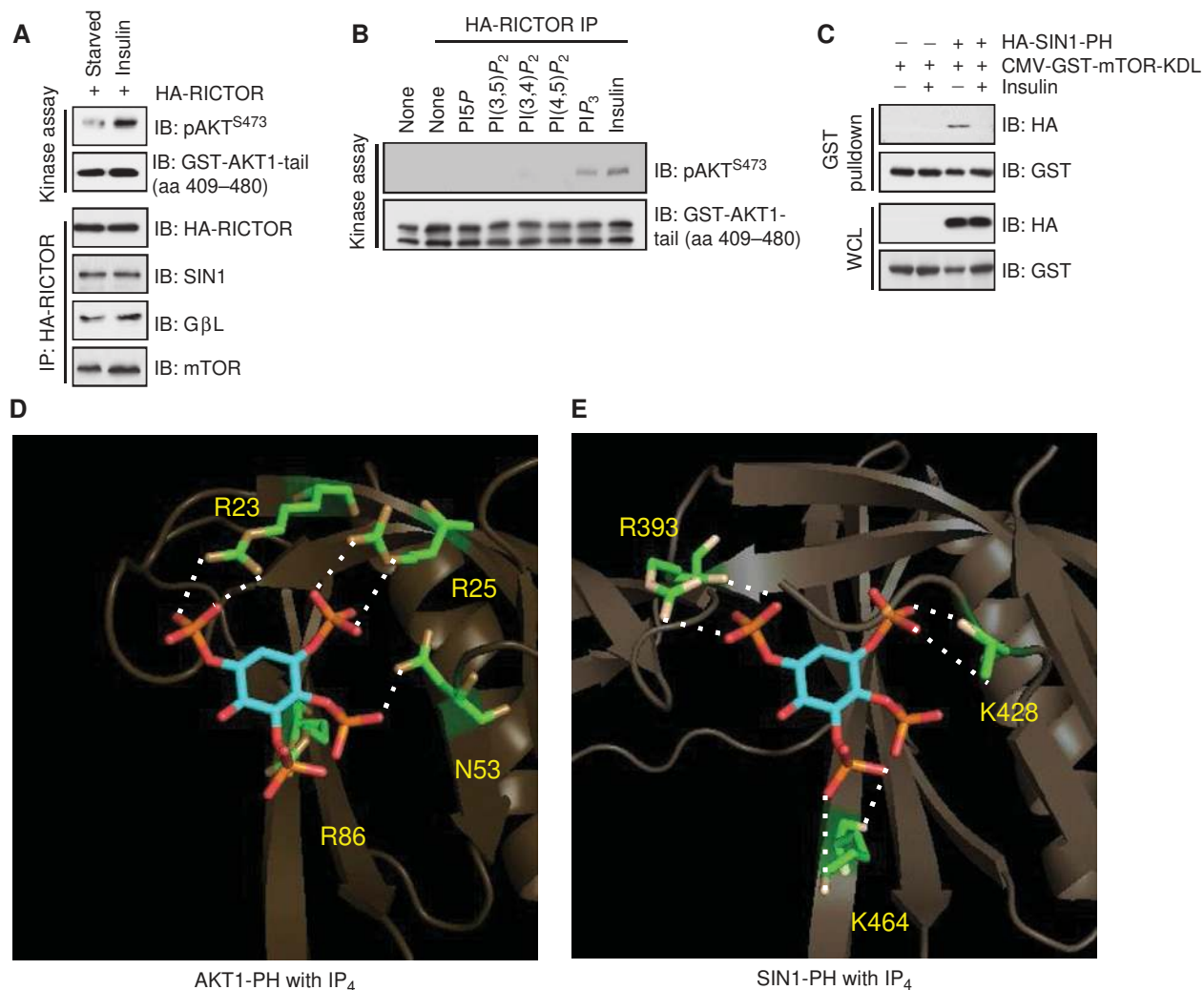


Figure 4. PI(3,4,5)P₃ promotes mTORC2 activation to phosphorylate AKT^{S473}. **A**, *in vitro* kinase assays indicating that mTORC2 complexes immunoprecipitated (IP) by HA-RICTOR are active upon insulin stimulation in phosphorylating AKT^{S473}. **B**, *in vitro* kinase assays showing that PI(3,4,5)P₃-polysomes activate the purified inactive mTORC2 complexes *in vitro*. HA-RICTOR-containing mTORC2 complexes were immunoprecipitated from HEK293 cells and serum starved for 36 hours before harvest in CHAPS buffers. Twenty-five microliters of 1 mmol/L polyPIP₃osomes containing 5% indicated PIP species were incubated with 10 μL of HA-RICTOR precipitates in kinase assays. **C**, insulin treatment attenuated SIN1-PH interaction with mTOR-KDL. Immunoblot (IB) analysis of whole cell lysates (WCL) and GST pulldowns derived from 293 cells transfected with indicated constructs. Where indicated, cells were serum starved for 24 hours and stimulated by 100 nmol/L insulin for 30 minutes before harvesting. **D**, an illustration of solved AKT1-PH/IP₄ cocrystal structure (PDB: 1UNQ) by PyMOL. **E**, an illustration of possible SIN1-PH/IP₄ complex structure by superimposing IP₄ into solved SIN1-PH structure (PDB: 3V0Q) by PyMOL.

by various SIN1 mutations (Supplementary Fig. S5C), suggesting that loss of PtdIns(3,4,5)P₃ binding (Figs. 3C and 5C) is the major reason for the failure of SIN1-CAA-containing mTORC2 complexes to phosphorylate AKT in cells (Fig. 5A and B and Supplementary Fig. S5A and S5B) and *in vitro* (Fig. 5D and Supplementary Fig. S5D). Notably, upon insulin stimulation, SIN1-CAA-expressing HAP1-*Sin1*^{-/-} cells displayed reduced pAKT^{S473}, but not a complete loss of pAKT^{S473} (Fig. 5B and Supplementary Fig. S5B), suggesting that in addition to PIP₃, other mechanisms may also account for mTORC2-mediated activation of AKT triggered by insulin, such as ribosome association with SIN1 (ref. 19; Supplementary Fig. S5E) or association with AKT that may bring mTORC2 to PM (27).

Moreover, compared with SIN1^{WT} (Supplementary Fig. S3F), the SIN1-CAA mutant displayed a significantly lower affinity with Ins(1,3,4,5)P₄ *in vitro* (Supplementary Fig. S5F), further supporting that R393, K428, and K464 may be the major residues that mediate SIN1-PH interaction with Ins(1,3,4,5)P₄. In agreement with this model, unlike SIN1-PH^{WT} (Fig. 2B–D), the PtdIns(3,4,5)P₃ binding-deficient SIN1-PH-CAA mutant was largely incapable of functionally substituting AKT1-PH to restore AKT phosphorylation in cells (Fig. 5E and Supplementary Fig. S5G and S5H). Furthermore, similar to SIN1-PH^{WT}, SIN1-PH-CAA largely retained its ability to bind mTOR-KD (Fig. 5F), thereby inhibiting mTOR-mediated phosphorylation of AKT^{S473} *in vitro* (Fig. 5G). Mechanistically, this may be in part due to

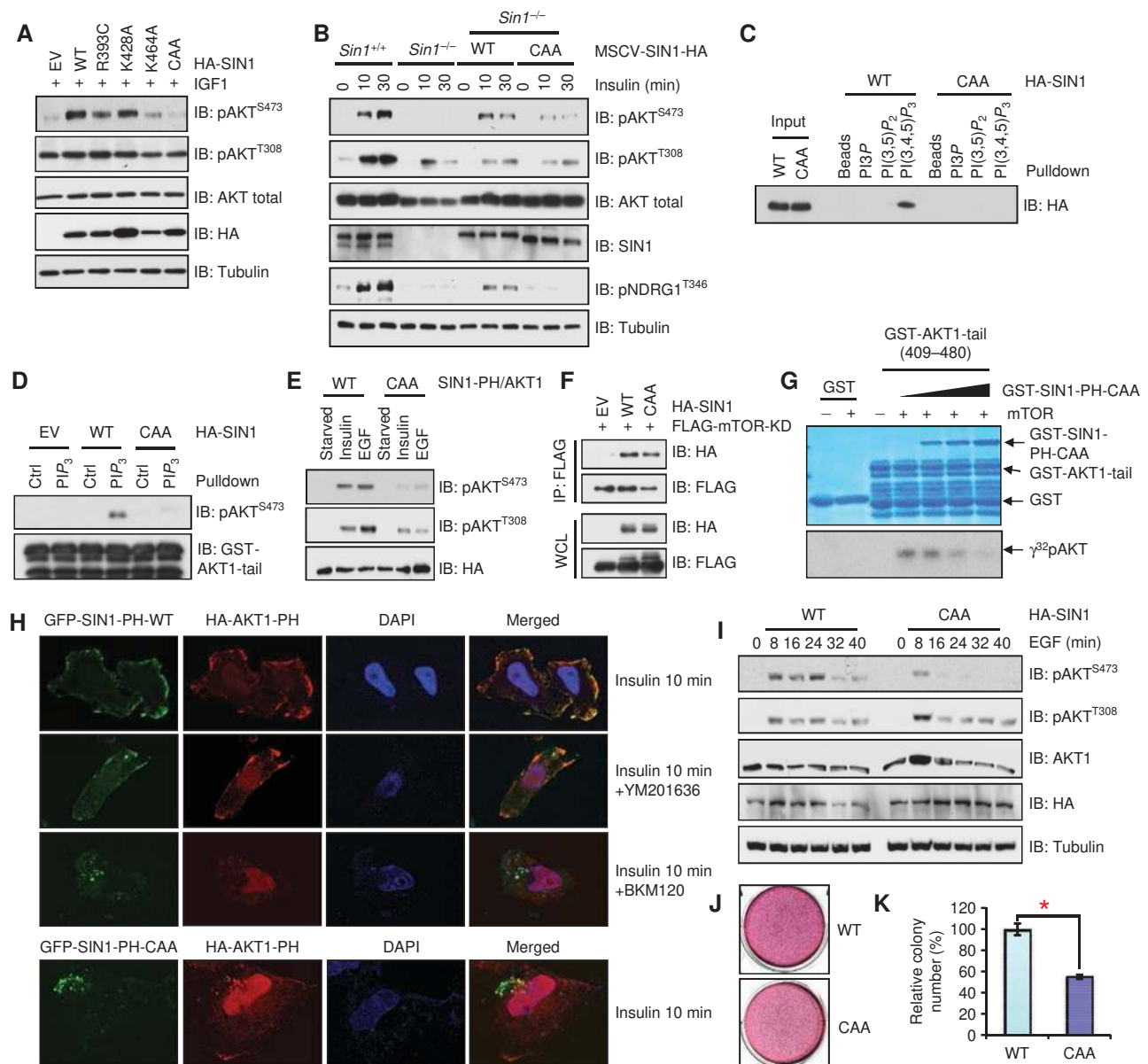


Figure 5. PI(3,4,5)P₃ mainly interacts with the SIN1-PH domain via R393, K428, and K464 residues to govern mTORC2 activation. **A**, the SIN1-R393C/K428A/K464A mutant is deficient in phosphorylating AKT^{S473}. Immunoblot (IB) analysis of whole cell lysates (WCL) derived from *Sin1*^{-/-} MEFs transfected with indicated constructs. Cells were serum starved for 24 hours before 100 ng/mL IGF1 was added for 30 minutes. **B**, SIN1-CAA is deficient in activating mTORC2 upon insulin stimulation. HAP1-*Sin1*^{-/-} cells were infected with MSCV-SIN1-HA-WT or CAA retroviruses, selected with 1 μg/mL puromycin for 3 days to eliminate noninfected cells and serum starved for 24 hours, and stimulated with 100 nmol/L insulin for indicated periods before harvesting for IB analyses. **C**, PI(3,4,5)P₃ loses its interaction with SIN1-CAA. IB of PIP₃ beads pull-downs derived from HEK293T cells transfected with indicated constructs. **D**, *in vitro* kinase assays demonstrating that PI(3,4,5)P₃ pulls down active mTORC2 complexes. IB of *in vitro* kinase assays derived from incubating PI(3,4,5)P₃ beads pull-downs from HEK293T cells transfected with indicated constructs, using GST-AKT1-tail (aa 409–480) as a substrate. **E**, SIN1-PH-CAA is deficient in functionally replacing AKT1-PH. IB analyses of WCLs derived from *Akt1*^{2-/-} MEFs transfected with indicated constructs. Where indicated, cells were serum starved for 36 hours before being stimulated by insulin (100 nmol/L) for 30 minutes or EGF (100 ng/mL) for 10 minutes. **F**, SIN1-CAA binds the mTOR kinase domain. IB analysis of HA-IPs and WCLs derived from HEK293T cells transfected with indicated constructs. **G**, SIN1-PH-CAA retains its ability to suppress mTOR kinase *in vitro*. *In vitro* kinase assays of recombinant active mTOR kinases with GST-AKT1-tail (aa 409–480) as a substrate, in the presence of increasing doses of bacterially purified GST-SIN1-PH-CAA recombinant proteins. **H**, representative confocal images to illustrate that GFP-SIN1-PH-WT, but not GFP-SIN1-PH-CAA, enriches and colocalizes with AKT1-PH at PM proximity upon insulin (100 nmol/L) stimulation. **I**, SIN1-CAA is deficient in activating AKT in cells. IB analysis of WCLs derived from SIN1-depleted OVCAR5 cells stably expressing MSCV-SIN1-WT-HA or MSCV-SIN1-CAA-HA. Where indicated, cells were serum starved for 36 hours before stimulation by EGF (100 ng/mL) for 10 minutes. **J** and **K**, soft-agar assays using OVCAR5 cell lines generated in **I**. *, *P* < 0.05 (Student *t* test).

Downloaded from <http://aacrjournals.org/cancerdiscovery/article-pdf/5/11/1194/1716891/1194.pdf> by guest on 24 August 2022

compromised SIN1-PH-CAA colocalization with AKT1-PH on PM, due to its deficiency to properly interact with PtdIns(3,4,5) P_3 present on the PM (Fig. 5H and Supplementary Fig. S5I and S5J).

To further examine how loss of PtdIns(3,4,5) P_3 binding to SIN1 may influence mTORC2-mediated cellular responses, we stably expressed SIN1^{WT} or the SIN1-CAA mutant in OVCAR5 cells depleted of endogenous SIN1. Under these conditions, we found that mTORC2 activity was attenuated in SIN1-CAA-expressing cells, as indicated by reduced AKT^{S473} phosphorylation upon EGF (Fig. 5I) or insulin (Supplementary Fig. S5K) stimulation in SIN1-CAA-expressing cells. More importantly, SIN1-CAA-expressing cells also formed fewer colonies on soft agar (Fig. 5J and K), indicating that loss of PtdIns(3,4,5) P_3 binding leads to impaired mTORC2 kinase activity, which subsequently suppresses cell transformation phenotypes. Notably, expression of SIN1-CAA did not significantly affect the cellular responses to various DNA damaging agents inducing apoptotic drugs, such as doxorubicin and cisplatin (Supplementary Fig. S5L and S5M), suggesting that although AKT can be activated upon DNA damage (Supplementary Fig. S5N), possibly mediated through DNA-PK (39), this mechanism is likely to be independent of PI3K/PtdIns(3,4,5) P_3 -mediated mTORC2 activation.

PtdIns(3,4,5) P_3 Binds the PH Domain of SIN1 and Releases SIN1-PH-Mediated Inhibition on the mTOR Kinase Domain

Notably, mTOR-KD (Fig. 6A and Supplementary Fig. S1A) or mTOR-KDL (Supplementary Figs. S1A and S6A), but not the full-length mTOR (Fig. 6B), competed with PtdIns(3,4,5) P_3 for binding SIN1, suggesting that PtdIns(3,4,5) P_3 may directly bind SIN1-PH to release SIN1-PH inhibition on the mTOR catalytic domain, therefore exposing the mTOR active site to mTOR substrates. On the other hand, in addition to the mTOR-KD/SIN1-PH interaction, mTOR might have additional interactions with SIN1 either directly or indirectly through GβL or RICTOR, because SIN1-PH expression (Fig. 1F and Supplementary Fig. S1W) or PtdIns(3,4,5) P_3 interaction with SIN1-PH (Fig. 6B) does not disrupt the mTORC2 holo-enzyme complex. This model is further rein-

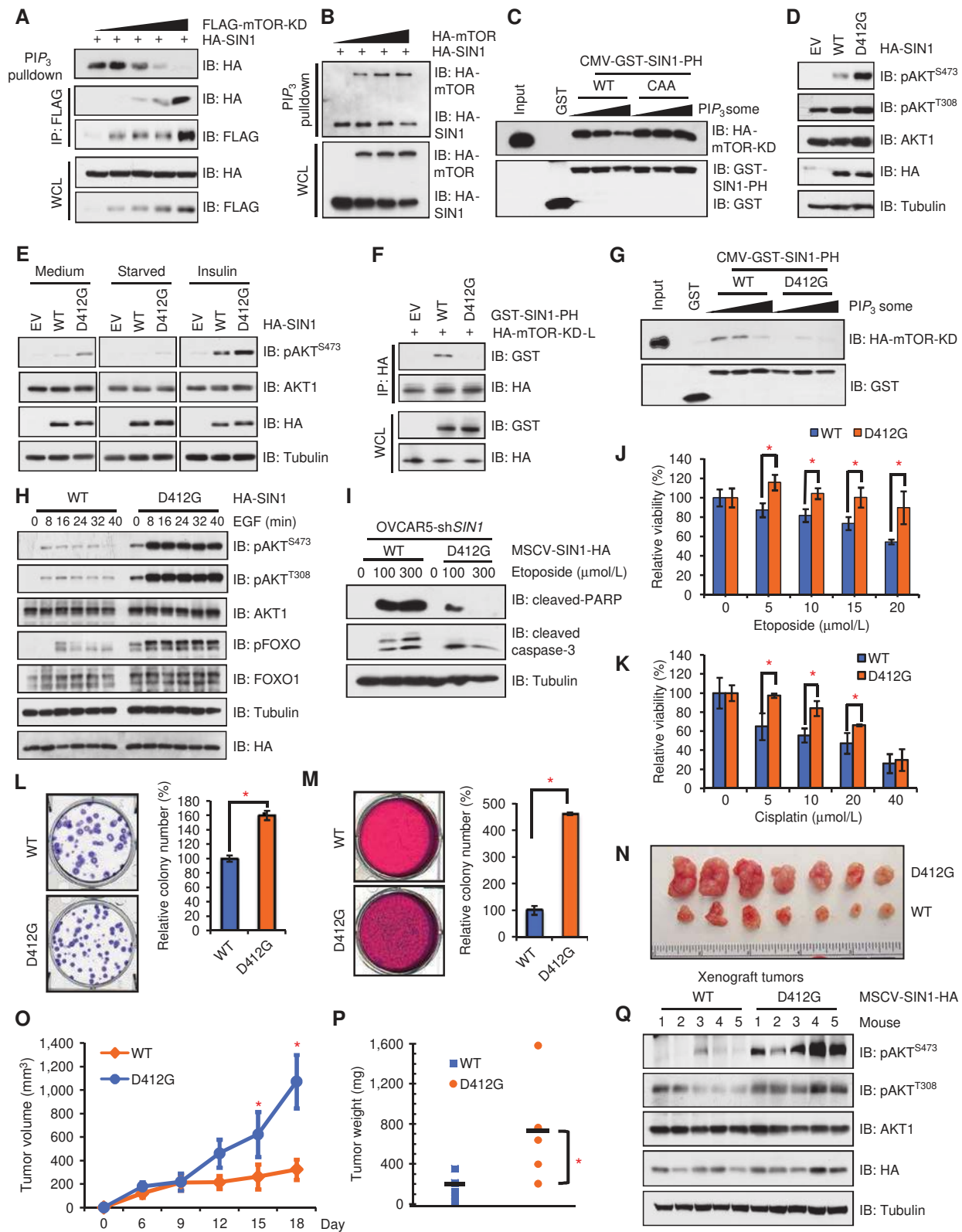
forced by the observation that PtdIns(3,4,5) P_3 -poly-PIPsomes gradually disturbed the mTOR-KD interaction with SIN1-PH^{WT}, but not SIN1-PH-CAA, in a dose-dependent manner (Fig. 6C). Notably, although SIN1-CAA is deficient in binding PtdIns(3,4,5) P_3 , it still binds mTOR-KD with a similar affinity to SIN1^{WT} (Fig. 5F). Together, these data indicate that both PtdIns(3,4,5) P_3 and mTOR-KD bind the SIN1-PH domain in a possibly mutually exclusive manner, such that PtdIns(3,4,5) P_3 binding releases SIN1-PH from binding the mTOR catalytic domain and activates mTORC2.

Cancer Patient-Derived Mutations in the PH Domain of SIN1 Display Elevated Oncogenic Ability to Activate AKT through Losing the SIN1-PH Interaction with the mTOR Kinase Domain

In order to pinpoint the SIN1-PH/mTOR-KD interaction patch, we examined cancer patient-derived SIN1-PH mutations, assuming that loss of the SIN1-PH/mTOR-KD interaction might lead to elevated AKT activation, thus facilitating tumorigenesis. Analysis of The Cancer Genome Atlas (TCGA) datasets (cBio and COSMIC) reveals 6 somatic mutations in the SIN1-PH domain (Supplementary Fig. S6B). Aside from two of these, most of the mutations in SIN1-PH compromised their interactions with mTOR-KD (Supplementary Fig. S6C), leading to elevated mTORC2 activity toward phosphorylating AKT^{Ser473} in cells (Supplementary Fig. S6D and S6E). Importantly, as the D412G mutant robustly enhanced mTORC2 activity to elevate AKT^{S473} phosphorylation in cells (Fig. 6D and E and Supplementary Fig. S6D and S6E), we chose this mutant for further mechanistic and functional studies.

Notably, compared with SIN1^{WT}, SIN1-D412G-containing mTORC2 complexes also exhibited elevated activity toward phosphorylating AKT *in vitro* under starved or normal conditions (Supplementary Fig. S6F), and this is in part due to its compromised binding to mTOR-KD (Fig. 6F and G). In addition, SIN1-D412G displayed enhanced mTORC2 kinase activity even under nonstimulated conditions (Fig. 6E and Supplementary Fig. S6F), suggesting that SIN1-D412G-containing mTORC2 may be more active through exposing the mTOR catalytic site. Collectively, these results reveal

Figure 6. PI(3,4,5) P_3 releases SIN1-PH-mediated inhibition on mTOR-KD, leading to mTORC2 activation. **A** and **B**, PI(3,4,5) P_3 competes with mTOR-KD (**A**), but not full-length mTOR (**B**) in binding SIN1. Immunoblot (IB) analysis of PIP₃ pull-downs, FLAG-immunoprecipitates (IP), and whole cell lysates (WCL) derived from HEK293T cells transfected with indicated constructs. **C**, PI(3,4,5) P_3 -polyosomes attenuate mTOR-KD interaction with SIN1-PH-WT, but not SIN1-PH-CAA. IB analysis of GST pull-downs in the presence of increasing amounts of PIP₃-polyosomes (0, 10, or 20 μ L) in CHAPS buffers. **D**, compared with SIN1^{WT}, ectopic expression of SIN1-D412G leads to elevated pAKT^{S473} in cells. IB analysis of WCLs derived from Sin1^{-/-} MEFs transfected with indicated SIN1 constructs. **E**, compared with SIN1^{WT}, ectopic expression of SIN1-D412G leads to elevated pAKT^{S473} under indicated experimental conditions. IB analysis of WCLs derived from Sin1^{-/-} MEFs transfected with indicated SIN1 constructs. Cells were serum starved for 24 hours before stimulation by insulin (100 nmol/L) for 30 minutes. **F** and **G**, SIN1-D412G loses interaction with mTOR-KD in cells (**F**) and *in vitro* (**G**). IB of HA-IPs and WCLs derived from HEK293T cells transfected with indicated constructs (**F**), or GST pull-downs in the presence of indicated PIP₃-polyosomes (**G**). **H**, compared with SIN1^{WT}, SIN1-D412G leads to an elevated AKT activation upon EGF stimulation. IB of WCLs derived from endogenous-SIN1-depleted OVCAR5 cells stably expressing indicated SIN1 constructs. Where indicated, cells were serum starved for 36 hours before stimulation by EGF (100 ng/mL) for 10 minutes. **I**, compared with SIN1^{WT}, SIN1-D412G results in reduced apoptosis. IB of WCLs derived from endogenous-SIN1-depleted OVCAR5 cells stably expressing indicated SIN1 constructs. Where marked, cells were treated with etoposide for 24 hours before collection. **J** and **K**, compared with SIN1^{WT}, SIN1-D412G-expressing cells display an elevated resistance to etoposide (**J**) or cisplatin (**K**) challenges. Various cell lines generated in **H** were cultured in 10% FBS-containing medium with the indicated concentrations of etoposide (**J**) or cisplatin (**K**) for 24 hours before performing cell viability assays. Data were shown as mean \pm SD for three independent experiments. *, $P < 0.05$ (Student t test). **L** and **M**, compared with SIN1^{WT}, SIN1-D412G-expressing cells display enhanced colony formation (**L**) and soft-agar growth abilities (**M**). Data were shown as mean \pm SD for three independent experiments. *, $P < 0.05$ (Student t test). **N-P**, compared with SIN1^{WT}, SIN1-D412G-expressing cells display enhanced tumor formation in a xenograft mouse model. 2.5×10^6 of the generated cells in (**H**) were injected into nude mice ($n = 10$ for each group) and monitored for tumor formation (**O**). Formed tumors were dissected (**N**) and weighed (**P**). As indicated, * represents $P < 0.05$ calculated by the Student t test. **Q**, compared with SIN1^{WT}, elevated AKT^{S473} levels were observed in SIN1-D412G-expressing xenograft tumors. IB analysis of WCLs derived from xenografted tumors obtained in **N**.



Downloaded from <http://aacrjournals.org/cancerdiscovery/article-pdf/5/11/1194/1716891/1194.pdf> by guest on 24 August 2022

the D412 residue as part of a critical binding patch for mediating SIN1-PH interactions with the mTOR catalytic domain, in a manner that is distinct from the SIN1-PH/PtdIns(3,4,5) P_3 -binding patch that includes R393, K428, and K464 (Fig. 4E).

To gain further insight into whether by losing inhibition of mTOR-KD, SIN1-D412G exerts oncogenic roles in cells via elevating mTOR kinase activity, we reintroduced SIN1-D412G or SIN1^{WT} in endogenous SIN1-depleted OVCAR5 ovarian cancer cells (Supplementary Fig. S6G), because this cancerous mutation was identified in an ovarian cancer patient (sample ID: TCGA-13-1509). Compared with SIN1^{WT}, SIN1-D412G-expressing cells displayed increased AKT phosphorylation (Fig. 6H) and correspondingly reduced cellular apoptosis triggered by etoposide (Fig. 6I), as well as enhanced resistance to chemotherapeutic drugs, such as etoposide (Fig. 6J and Supplementary Fig. S6H), cisplatin (Fig. 6K), doxorubicin (Supplementary Fig. S6I), or Taxol (Supplementary Fig. S6J). In addition to its antiapoptotic function, elevated AKT activity in SIN1-D412G-expressing cells also resulted in enhanced colony formation ability (Fig. 6L), soft-agar growth (Fig. 6M), and increased tumor growth in a xenograft assay (Fig. 6N–Q and Supplementary Fig. S6K). Furthermore, other SIN1-PH cancerous mutations, including S449I, A451E, and T456M, that displayed significantly reduced interactions with mTOR-KD (Supplementary Fig. S6C) also exhibited elevated and sustained AKT activation (Supplementary Fig. S6L and S6M), as well as enhanced colony formation and soft-agar growth ability (Supplementary Fig. S6N–S6Q). These results together support a model in which these SIN1-PH mutants may form a critical SIN1-PH/mTOR-KD interaction patch, and they are more oncogenic than SIN1^{WT}, in part due to elevated mTORC2/AKT oncogenic signaling resulting from their loss of inhibitory effects on mTOR-KD.

This is corroborated by depletion of endogenous AKT1 (Supplementary Fig. S6R) or AKT2 (Supplementary Fig. S6S) in SIN1-D412G-expressing OVCAR5 cells, which sensitized cells to treatments with chemotherapeutic drugs, including cisplatin (Supplementary Fig. S6T) and doxorubicin (Supplementary Fig. S6U), as well as reduced colony formation (Supplementary Fig. S6V) and soft-agar growth (Supplementary Fig. S6W). Notably, compared with SIN1^{WT}, expression of SIN1-D412G did not lead to significant changes in cell-cycle profiles (Supplementary Fig. S6X–S6Z), highlighting that the oncogenic activity of SIN1-D412G is largely due to direct activation of mTORC2, rather than a secondary cell-cycle effect (40), to augment AKT oncogenic signaling.

Addition of the KRAS-CAAX Sequence to the Carboxyl-Terminus of SIN1 Generates a Relatively Constitutively Active mTORC2

Intrigued by the fact that membrane-targeted AKT mutants are constitutively active (41), analogously we generated two putative constitutively active SIN1 mutants, one with a SRC myristoylation (MYR) tag at the N-terminus and the other one fused in frame with a KRAS-CAAX motif at the carboxyl-terminus immediately after its PH motif (Fig. 7A), because the CAAX motif at the C-terminus of RAS creates a farnesyl moiety necessary for RAS membrane association and activation (42).

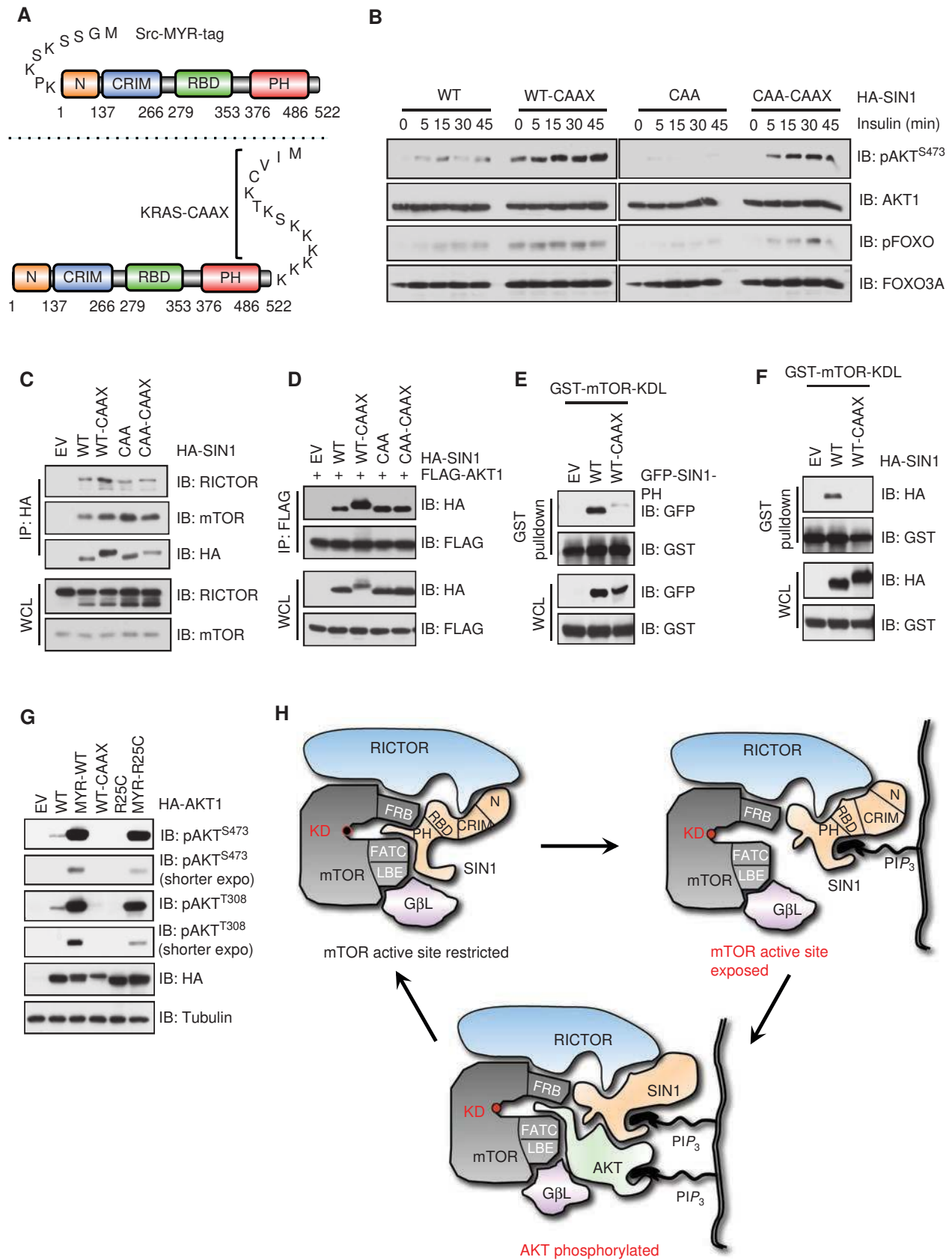
Notably, the SIN1-CAAX mutant, but not the MYR-SIN1 mutant, led to elevated mTORC2 activity in transfected cells (Supplementary Fig. S7A), and in part rescued SIN1-CAA toward phosphorylating AKT in cells (Fig. 7B) and *in vitro* (Supplementary Fig. S7B), suggesting that spatially, C-terminal rather than N-terminal attachment of SIN1 to PM is critical for activating mTORC2. Moreover, the CAAX moiety did not influence mTORC2 complex integrity (Fig. 7C) or interaction with its substrate AKT (Fig. 7D), but in part attenuated the inhibitory binding of SIN1-PH to mTOR-KD (Fig. 7E and F), supporting the notion that the C-terminal CAAX tag could in part compensate for the loss of PtdIns(3,4,5) P_3 binding in the SIN1-CAA mutant, mainly through both releasing SIN1-PH-mediated inhibition on mTOR-KD and directly recruiting the SIN1 to PM (Supplementary Fig. S5J and Supplementary Fig. S7C and S7D). Similarly, the addition of an N-terminal MYR-tag to AKT1 largely rescued phosphorylation of the PtdIns(3,4,5) P_3 binding-deficient AKT1^{R25C} mutant (Fig. 7G), whereas the C-terminal tagging of a CAAX sequence completely abrogated AKT activity, likely interfering with phosphorylation of the C-terminus of AKT (ref. 40; Fig. 7G and Supplementary Fig. S7E). Thus, similar to MYR-AKT, SIN1-CAAX could in part functionally phosphorylate AKT^{S473} independent of PI(3,4,5) P_3 (Supplementary Fig. S7F and S7G).

Collectively, our results support a model in which the SIN1-PH domain interacts with and inhibits the mTOR kinase domain, and the direct binding of PtdIns(3,4,5) P_3 with the SIN1-PH motif releases the inhibitory effect of SIN1, leading to mTORC2 activation and AKT phosphorylation (Fig. 7H).

DISCUSSION

Although hyperactivation of the mTORC2–AKT pathway has been commonly observed in various human cancers (43, 44), where and how the mTORC2 kinase complex is

Figure 7. C-terminal tagging of the KRAS-CAAX sequence to SIN1 partially rescues the deficiency of SIN1-CAA toward activating AKT. **A**, schematic illustration of the MYR-SIN1 or SIN1-CAAX chimera structure. **B**, C-terminal addition of the KRAS-CAAX sequence in part rescues SIN1-CAA in phosphorylating AKT^{S473} in cells. Immunoblot (IB) analysis of whole cell lysates (WCL) derived from *Sin1*^{-/-} MEFs transfected with indicated constructs. Where indicated, cells were serum starved for 24 hours and stimulated by 100 nmol/L insulin for indicated time periods. **C** and **D**, addition of KRAS-CAAX sequence does not affect mTORC2 complex integrity (**C**) or SIN1 interaction with AKT1 (**D**). IB of FLAG-IPs and WCLs derived from 293T cells transfected with indicated constructs. **E** and **F**, the CAAX tag alleviates SIN1-PH interaction with mTOR-KD. IB of GST pull-downs and WCLs derived from 293T cells transfected with indicated constructs. **G**, addition of an N-terminal-MYR tag, but not a C-terminal-CAAX tag, largely rescues AKT phosphorylation in AKT1^{R25C} mutant. IB analysis of WCLs derived from DLD1-AKT1/2^{-/-} cells transfected with indicated constructs. **H**, a proposed model for the PI(3,4,5) P_3 -mediated mTORC2 activation mechanism.



Downloaded from <http://aacrjournals.org/cancerdiscovery/article-pdf/5/11/1194/1716891/1194.pdf> by guest on 24 August 2022

activated upon growth stimulation has remained elusive for decades. Distinct from mTORC1 that depends on proteins including RAG GTPase and RHEB GTPase for lysosomal recruitment and activation (12), in this study we identified a nonprotein molecule PtdIns(3,4,5) P_3 as a direct upstream activator for mTORC2. Mechanistically, consistent with the crystal insights from the partially active mTOR complex (21), the active site of mTOR in the mTORC2 complex is largely governed by the PH domain of SIN1, and the binding of SIN1-PH to mTOR-KD under nonstimulated conditions blocks the access of the mTORC2 substrate AKT to the mTOR active site for phosphorylation and activation. Upon insulin or growth stimulation, activated PI3K generates PtdIns(3,4,5) P_3 that directly binds SIN1-PH in part via R393, K428, and K464 residues, leading to attenuated SIN1-PH interaction with the mTOR kinase domain and subsequent exposure of the mTOR active site to AKT for its activation. Given that SIN1 is also the mTORC2 component responsible for recruiting certain mTORC2 substrates, including SGK and AKT (45), it seems that SIN1 plays dual roles in mediating AKT activation by mTORC2: SIN1 controls the timing of the exposure of the mTOR catalytic core and spatially recruits AKT to mTORC2 complex proximity for AKT^{S473} phosphorylation and activation. However, the detailed molecular mechanisms underlying how these two events are coordinated warrant further investigation.

Interestingly, cancer patient-derived SIN1 oncogenic mutations (D412G characterized in this study and R81T characterized in ref. 28) appear to be mutually exclusive with either *AKT1* gene amplification (Supplementary Fig. S7H) or *PIK3CA* oncogenic mutations (E545K and H1047R; ref. 46; Supplementary Fig. S7I). These observations support that PI3K/SIN1/AKT may be in the same genetic pathway, highlighting the critical role of PI3K in governing mTORC2 activation. As previously ribosome association has been shown to be critical for mTORC2 activation (19), and mTORC2 was observed at various cellular components, including the nucleus, mitochondria, ER, and PM (17), whether there are populations of mTORC2 subcomplexes at various cellular locations, as well as how and whether mTORC2 shuttles between ribosomes and PM or other cellular components for activation, warrant further exploration. Interestingly, two recent studies suggest that both mTORC2 and mTORC1 form dimers for function (27, 47), echoing previous discoveries in yeast that yeast TOR complexes are dimers (48). Consistently, dimerization of other members of the PIKK superfamilies, including DNA-PK (49) and ATM (50), have been observed and shown to be critical for their activation. This dimerization or even oligomerization feature for the mTOR complex potentially adds additional layers of regulations for the mechanistic studies, which may require a patch of phospholipids, or lipid rafts enriched with PtdIns(3,4,5) P_3 to hook mTORC2 for activation.

METHODS

Cell Lines

All cells were maintained in DMEM or RPMI supplemented with 10% FBS and 100 U/mL penicillin and streptomycin. HAP1-*Sin1*^{-/-} and matching parental cells were purchased from Horizon in June

2015. All other cell lines were routinely maintained and examined in the lab but have not been further authenticated.

Cell Culture

Cell transfection was performed using lipofectamine and plus reagents as described previously (40). Packaging of lentiviral shRNA viruses and retroviral MSCV-SIN1-expressing viruses, as well as subsequent infection of various cell lines, was performed according to the protocol described previously (51). Kinase inhibitors wortmannin (Selleck; S2758), LY2940002 (Cell Signaling Technology; 9901), PLK90 (a kind gift from the Shepherd Lab), BKM120 (Selleck; S2247), and YM201636 (Santa Cruz; SC 204193) were used at the dose as indicated. PIP strips (P6001), PIP-polysomes (Y0000, Y-P0000, Y-P0003, Y-P0004, Y-P0005, Y-P034, Y-P0035, Y-P0039, and Y-P045), and PIP beads (P-B00Ss) were purchased from Echelon Biosciences. EGF (Sigma; E9644), insulin (Invitrogen; 41400-045), IGF1 (Sigma; I3769), etoposide (Sigma; E1383), cisplatin (Selleck; S1166), doxorubicin (Sigma; D1515), and taxol (Sigma; T7191) were used at the indicated doses.

Antibodies

All antibodies were used at a 1:1,000 dilution in 5% nonfat milk for Western blotting. Anti-phospho-Ser473-AKT antibody (mouse mAb 4051 and rabbit mAb 4060), anti-phospho-Thr308-AKT antibody (2965), anti-phospho-Thr450-AKT antibody (12178), anti-AKT1 antibody (2938), anti-AKT total antibody (4691), anti-phospho-Ser9-GSK3 β antibody (5558), anti-GSK3 β antibody (12456), anti-RICTOR antibody (9476), anti-mTOR antibody (2983), anti-G β L antibody (3274), anti-SIN1 antibody (12860 or K87 generated in the Su lab), anti-phospho-NDRG1 (3217), anti-phospho-FOXO1(Thr24)/FOXO3a(Thr32) antibody (9464), anti-FOXO1 antibody (9454), anti-phospho-T246-PRAS40 antibody (13175), anti-PRAS40 antibody (2691), anti-PIK3CA (p110 α) antibody (4249), anti-GST antibody (2625), polyclonal anti-MYC-Tag antibody (2278), monoclonal anti-MYC-Tag (2276), anti-cleaved PARP antibody (5625), and anti-cleaved caspase-3 antibody (9661) were purchased from Cell Signaling Technology. Polyclonal anti-HA antibody (sc-805) was purchased from Santa Cruz. Anti-tubulin antibody (T-5168), anti-vinculin antibody (V-4505), polyclonal anti-FLAG antibody (F-2425), monoclonal anti-FLAG antibody (F-3165, clone M2), anti-FLAG agarose beads (A-2220), anti-HA agarose beads (A-2095), peroxidase-conjugated anti-mouse secondary antibody (A-4416), and peroxidase-conjugated anti-rabbit secondary antibody (A-4914) were purchased from Sigma. Monoclonal anti-HA antibody (901502) was purchased from BioLegend. The anti-phospho-Ser657-PKC antibody (sc-12356) was purchased from Santa Cruz Biotechnology. The anti-PIKFYVE antibody was generated by Cell Signaling Technology.

PIP Strip Overlay Assays

The overlay assays were performed according to the manufacturer's instructions with minor modifications. Briefly, PIP membranes were blocked with 3% BSA in 1 \times TBST (0.1% Tween-20) at room temperature for 1 hour. Two μ g/mL purified GST or GST-SIN1 proteins were incubated with PIP membranes at room temperature for another 2 hours, followed by gentle washing in 1 \times TPST for 3 \times 5 minutes. Anti-GST antibody (1:1,000 from CST 2625) was prepared in 3% BSA in 1 \times TBST and incubated with the membranes for 1 hour at room temperature. After gentle washing in 1 \times TPST for 3 \times 5 minutes, membranes were subjected to Western blotting.

Immunoblots and Immunoprecipitation

Cells were lysed as indicated in EBC buffer (50 mmol/L Tris, pH 7.5, 120 mmol/L NaCl, 0.5% NP-40) or CHAPS (50 mmol/L Tris,

pH 7.5, 120 mmol/L NaCl, 0.3% CHAPS) supplemented with protease inhibitors (Complete Mini, Roche) and phosphatase inhibitors (phosphatase inhibitor cocktail set I and II, Calbiochem). The protein concentrations of lysates were measured by the Beckman Coulter DU-800 spectrophotometer using the Bio-Rad protein assay reagent. The same amounts of whole cell lysates were resolved by SDS-PAGE and immunoblotted with the indicated antibodies. For immunoprecipitation, 1,000 µg lysates were incubated with the indicated antibody (1–2 µg) for 3 to 4 hours at 4°C followed by 1-hour incubation with Protein A/G sepharose beads (GE Healthcare). Immunoprecipitants were washed five times with NETN buffers (20 mmol/L Tris, pH 8.0, 100 mmol/L NaCl, 1 mmol/L EDTA, and 0.5% NP-40) or CHAPS buffers before being resolved by SDS-PAGE and immunoblotted with indicated antibodies.

In Vitro Kinase Assays

mTOR *in vitro* kinase assays were adapted as described previously (40). Briefly, the reaction contains 100 ng mTOR (EMD/Calbiochem 475987, contains truncated mTOR kinase domain with amino acids 1360–2549), 2 µg of GST or GST-AKT1-tail (aa 409–480), and 100 µmol/L cold ATP (with 1 µCi/mL γ -³²P-ATP for hot assays) in the kinase assay buffers (50 µmol/L HEPES, pH 7.5, 10 µmol/L MnCl₂, 10 µmol/L MgCl₂, 2 µmol/L DTT, and 0.5 µmol/L EGTA). As illustrated in the figures, indicated amounts of GST or GST-SIN1-PH recombinant proteins were added to the reactions for competition assays. The reactions were incubated at 30°C for 30 minutes. The reaction was stopped by the addition of SDS-containing lysis buffer and resolved by SDS-PAGE. Phosphorylation of GST-AKT1-tail was detected by autoradiography.

mTORC2 *in vitro* kinase assays were performed as described below. Briefly, HA immunoprecipitation in CHAPS buffer was performed in HEK293 cells transfected with HA-RICTOR under serum starvation (for 48 hours) or insulin stimulation (100 nmol/L insulin for 30 minutes) conditions. HA-RICTOR immunoprecipitates (IP) were washed extensively in CHAPS buffer and supplied as the kinase sources for *in vitro* kinase assays. HA-RICTOR IPs (10 µL) were incubated with 2 µg of GST-AKT1-tail (aa 409–480) and 200 µmol/L cold ATP in the kinase assay buffer (50 µmol/L HEPES, pH 7.5, 10 µmol/L MnCl₂, 10 µmol/L MgCl₂, 2 µmol/L DTT, 0.5 µmol/L EGTA), in the presence of indicated amount of PIP-polysomes at 30°C for 1 hour. The reactions were gently tapped every 10 minutes to mix the reactions well, and the reactions were stopped by the addition of SDS-containing lysis buffer and resolved by SDS-PAGE. Phosphorylation of GST-AKT1-tail was detected by Western blotting using the pAKT^{S473} antibody.

Immunofluorescence and Confocal Analysis

Cells were grown on glass coverslips for 24 hours and fixed with 3.7% formaldehyde in 1× PBS for 15 minutes at room temperature and permeabilized with 0.1% Triton X-100 in 1× PBS for 5 minutes. Samples were rinsed three times in 1× PBS with 5 minutes each wash. Coverslips were then blocked for 30 minutes with 5% BSA and incubated with primary antibodies for 60 minutes. After 3 × 5 minute, 1× PBST (0.1% Tween-20) washes, the coverslips were incubated with Alexa-488-conjugated goat anti-Rabbit secondary antibody or Alexa-594-conjugated goat anti-mouse secondary antibody (Invitrogen) for 60 minutes and washed three times with 1× PBST. Nuclei were counterstained with 4,6-diamidino-2-phenylindole (DAPI) for 10 minutes. Coverslips were rinsed 2 × 3 minutes with 1× PBS and mounted onto slides using prolong gold anti-fade reagent (Invitrogen).

Mouse Xenograft Assays

All animal experiments were approved by the Beth Israel Deaconess Medical Center International Animal Care and Use Committee review board. Briefly, 2.5 × 10⁶ endogenous SIN1-depleted OVCAR5 cells stably expressing MSCV-SIN1-WT-HA or MSCV-SIN1-D412G-HA were

mixed with Matrigel (1:1) and injected into the flank of 10 female nude mice (5 weeks old). Tumor size was measured every 3 days with a caliper, and the tumor volume was determined with the formula $L \times W^2 \times 0.52$, where L is the longest diameter and W is the shortest diameter. After 18 days, mice were sacrificed and xenografted solid tumors were dissected, then tumor weights were measured and recorded.

Disclosure of Potential Conflicts of Interest

L.C. Cantley is a consultant/advisory board member for GSK, Novartis, and Pfizer. W. Wei is a consultant/advisory board member for Cell Signaling Technology. No potential conflicts of interest were disclosed by the other authors.

One of the Editors-in-Chief is an author on this article. In keeping with the AACR's editorial policy, the peer review of this submission was managed by a senior member of *Cancer Discovery's* editorial team; a member of the AACR Publications Committee rendered the final decision concerning acceptability.

Authors' Contributions

Conception and design: P. Liu, A. Toker, B. Su, W. Wei
Development of methodology: P. Liu, B. Su, W. Wei
Acquisition of data (provided animals, acquired and managed patients, provided facilities, etc.): P. Liu, Y.R. Chin, J. Zhang, B. Wang, J. Blenis
Analysis and interpretation of data (e.g., statistical analysis, biostatistics, computational analysis): P. Liu, Y.R. Chin, K. Ogura, B. Su, W. Wei
Writing, review, and/or revision of the manuscript: P. Liu, W. Gan, Y.R. Chin, J. Guo, J. Zhang, J. Blenis, L.C. Cantley, A. Toker, B. Su, W. Wei
Administrative, technical, or material support (i.e., reporting or organizing data, constructing databases): W. Gan, W. Wei
Study supervision: L.C. Cantley, W. Wei

Acknowledgments

The authors thank Hiroyuki Inuzuka, Brian North, Alan W. Lau, Lixin Wan, and other Wei laboratory members for critical reading of the manuscript, and members of the Wei, Su, Cantley, Blenis, and Toker laboratories for helpful discussions. They also thank Dr. E. Emrah Er for sharing critical PIKfyve-related reagents and Dr. Emilie Clement for sharing various PI3K inhibitors and PIK3CA shRNAs. They also sincerely thank Dr. Mark A. Lemmon (Yale University) for critical help and suggestions.

Grant Support

W. Wei is an American Cancer Society research scholar. P. Liu is supported by 1K99CA181342 from the National Cancer Institute. This work was supported in part by NIH grants (R01CA177910, to W. Wei and A. Toker; R01GM094777, to W. Wei; R00CA157945, to Y.R. Chin; and R01GM041890, to L.C. Cantley).

Received April 18, 2013; revised August 14, 2015; accepted August 18, 2015; published OnlineFirst August 20, 2015.

REFERENCES

- Laplanche M, Sabatini DM. mTOR signaling in growth control and disease. *Cell* 2012;149:274–93.
- Kim DH, Sarbassov DD, Ali SM, King JE, Latek RR, Erdjument-Bromage H, et al. mTOR interacts with raptor to form a nutrient-sensitive complex that signals to the cell growth machinery. *Cell* 2002; 110:163–75.
- Sarbassov DD, Ali SM, Kim DH, Guertin DA, Latek RR, Erdjument-Bromage H, et al. Rictor, a novel binding partner of mTOR, defines

- a rapamycin-insensitive and raptor-independent pathway that regulates the cytoskeleton. *Curr Biol* 2004;14:1296–302.
4. Yang Q, Inoki K, Ikenoue T, Guan KL. Identification of Sin1 as an essential TORC2 component required for complex formation and kinase activity. *Genes Dev* 2006;20:2820–32.
 5. Jacinto E, Facchinetti V, Liu D, Soto N, Wei S, Jung SY, et al. SIN1/MIP1 maintains rictor-mTOR complex integrity and regulates Akt phosphorylation and substrate specificity. *Cell* 2006;127:125–37.
 6. Frias MA, Thoreen CC, Jaffe JD, Schroder W, Sculley T, Carr SA, et al. mSin1 is necessary for Akt/PKB phosphorylation, and its isoforms define three distinct mTORC2s. *Curr Biol* 2006;16:1865–70.
 7. Wang S, Tsun ZY, Wolfson RL, Shen K, Wyant GA, Plovanich ME, et al. Metabolism. Lysosomal amino acid transporter SLC38A9 signals arginine sufficiency to mTORC1. *Science* 2015;347:188–94.
 8. Rebsamen M, Pochini L, Stasyk T, de Araujo ME, Galluccio M, Kandasamy RK, et al. SLC38A9 is a component of the lysosomal amino acid sensing machinery that controls mTORC1. *Nature* 2015;519:477–81.
 9. Sancak Y, Peterson TR, Shaul YD, Lindquist RA, Thoreen CC, Bar-Peled L, et al. The Rag GTPases bind raptor and mediate amino acid signaling to mTORC1. *Science* 2008;320:1496–501.
 10. Bar-Peled L, Schweitzer LD, Zoncu R, Sabatini DM. Ragulator is a GEF for the rag GTPases that signal amino acid levels to mTORC1. *Cell* 2012;150:1196–208.
 11. Zoncu R, Bar-Peled L, Efeyan A, Wang S, Sancak Y, Sabatini DM. mTORC1 senses lysosomal amino acids through an inside-out mechanism that requires the vacuolar H(+)-ATPase. *Science* 2011;334:678–83.
 12. Bar-Peled L, Sabatini DM. Regulation of mTORC1 by amino acids. *Trends Cell Biol* 2014;24:400–6.
 13. Inoki K, Li Y, Xu T, Guan KL. Rheb GTPase is a direct target of TSC2 GAP activity and regulates mTOR signaling. *Genes Dev* 2003;17:1829–34.
 14. Ma L, Chen Z, Erdjument-Bromage H, Tempst P, Pandolfi PP. Phosphorylation and functional inactivation of TSC2 by Erk implications for tuberous sclerosis and cancer pathogenesis. *Cell* 2005;121:179–93.
 15. Inoki K, Ouyang H, Zhu T, Lindvall C, Wang Y, Zhang X, et al. TSC2 integrates Wnt and energy signals via a coordinated phosphorylation by AMPK and GSK3 to regulate cell growth. *Cell* 2006;126:955–68.
 16. Jewell JL, Kim YC, Russell RC, Yu FX, Park HW, Plouffe SW, et al. Metabolism. Differential regulation of mTORC1 by leucine and glutamine. *Science* 2015;347:194–8.
 17. Betz C, Hall MN. Where is mTOR and what is it doing there? *J Cell Biol* 2013;203:563–74.
 18. Zoncu R, Efeyan A, Sabatini DM. mTOR: from growth signal integration to cancer, diabetes and ageing. *Nat Rev Mol Cell Biol* 2011;12:21–35.
 19. Zinzalla V, Stracka D, Oppliger W, Hall MN. Activation of mTORC2 by association with the ribosome. *Cell* 2011;144:757–68.
 20. Oh WJ, Wu CC, Kim SJ, Facchinetti V, Julien LA, Finlan M, et al. mTORC2 can associate with ribosomes to promote cotranslational phosphorylation and stability of nascent Akt polypeptide. *EMBO J* 2010;29:3939–51.
 21. Yang H, Rudge DG, Koos JD, Vaidialingam B, Yang HJ, Pavletich NP. mTOR kinase structure, mechanism and regulation. *Nature* 2013;497:217–23.
 22. Alessi DR, Kulathu Y. Structural biology: security measures of a master regulator. *Nature* 2013;497:193–4.
 23. Sauer E, Imseng S, Maier T, Hall MN. Conserved sequence motifs and the structure of the mTOR kinase domain. *Biochem Soc Trans* 2013;41:889–95.
 24. Cheng J, Zhang D, Kim K, Zhao Y, Zhao Y, Su B. Mip1, an MEKK2-interacting protein, controls MEKK2 dimerization and activation. *Mol Cell Biol* 2005;25:5955–64.
 25. Schroder W, Bushell G, Sculley T. The human stress-activated protein kinase-interacting 1 gene encodes JNK-binding proteins. *Cell Signal* 2005;17:761–7.
 26. Schroder WA, Buck M, Cloonan N, Hancock JF, Suhrbier A, Sculley T, et al. Human Sin1 contains Ras-binding and pleckstrin homology domains and suppresses Ras signalling. *Cell Signal* 2007;19:1279–89.
 27. Gaubitz C, Oliveira TM, Prouteau M, Leitner A, Karuppasamy M, Konstantinidou G, et al. Molecular basis of the rapamycin insensitivity of target of rapamycin complex 2. *Mol Cell* 2015;58:977–88.
 28. Liu P, Gan W, Inuzuka H, Lazorchak AS, Gao D, Arojo O, et al. Sin1 phosphorylation impairs mTORC2 complex integrity and inhibits downstream Akt signalling to suppress tumorigenesis. *Nat Cell Biol* 2013;15:1340–50.
 29. Liu P, Guo J, Gan W, Wei W. Dual phosphorylation of Sin1 at T86 and T398 negatively regulates mTORC2 complex integrity and activity. *Protein Cell* 2014;5:171–7.
 30. Lemmon MA. Pleckstrin homology (PH) domains and phosphoinositides. *Biochem Soc Symp* 2007;81–93.
 31. Gao D, Wan L, Inuzuka H, Berg AH, Tseng A, Zhai B, et al. Rictor forms a complex with Cullin-1 to promote SGK1 ubiquitination and destruction. *Mol Cell* 2010;39:797–808.
 32. Franke TF, Kaplan DR, Cantley LC, Toker A. Direct regulation of the Akt proto-oncogene product by phosphatidylinositol-3,4-bisphosphate. *Science* 1997;275:665–8.
 33. Zolov SN, Bridges D, Zhang Y, Lee WW, Riehle E, Verma R, et al. In vivo, Pikfyve generates PI(3,5)P2, which serves as both a signaling lipid and the major precursor for PI3P. *Proc Natl Acad Sci U S A* 2012;109:17472–7.
 34. Poston CN, Duong E, Cao Y, Bazemore-Walker CR. Proteomic analysis of lipid raft-enriched membranes isolated from internal organelles. *Biochem Biophys Res Commun* 2011;415:355–60.
 35. Berchtold D, Piccolis M, Chiaruttini N, Riezman I, Riezman H, Roux A, et al. Plasma membrane stress induces relocalization of Slm proteins and activation of TORC2 to promote sphingolipid synthesis. *Nat Cell Biol* 2012;14:542–7.
 36. Wedaman KP, Reinke A, Anderson S, Yates J 3rd, McCaffery JM, Powers T. Tor kinases are in distinct membrane-associated protein complexes in *Saccharomyces cerevisiae*. *Mol Biol Cell* 2003;14:1204–20.
 37. Gan X, Wang J, Su B, Wu D. Evidence for direct activation of mTORC2 kinase activity by phosphatidylinositol 3,4,5-trisphosphate. *J Biol Chem* 2011;286:10998–1002.
 38. Pan D, Matsuura Y. Structures of the pleckstrin homology domain of *Saccharomyces cerevisiae* Avo1 and its human orthologue Sin1, an essential subunit of TOR complex 2. *Acta Crystallogr Sect F Struct Biol Cryst Commun* 2012;68:386–92.
 39. Bozulic L, Surucu B, Hynx D, Hemmings BA. PKBalpha/Akt1 acts downstream of DNA-PK in the DNA double-strand break response and promotes survival. *Mol Cell* 2008;30:203–13.
 40. Liu P, Begley M, Michowski W, Inuzuka H, Ginzberg M, Gao D, et al. Cell-cycle-regulated activation of Akt kinase by phosphorylation at its carboxyl terminus. *Nature* 2014;508:541–5.
 41. Kohn AD, Takeuchi F, Roth RA. Akt, a pleckstrin homology domain containing kinase, is activated primarily by phosphorylation. *J Biol Chem* 1996;271:21920–6.
 42. Ahearn IM, Haigis K, Bar-Sagi D, Philips MR. Regulating the regulator: post-translational modification of RAS. *Nat Rev Mol Cell Biol* 2012;13:39–51.
 43. Guertin DA, Sabatini DM. Defining the role of mTOR in cancer. *Cancer Cell* 2007;12:9–22.
 44. Inoki K, Corradetti MN, Guan KL. Dysregulation of the TSC-mTOR pathway in human disease. *Nat Genet* 2005;37:19–24.
 45. Cameron AJ, Linch MD, Saurin AT, Escribano C, Parker PJ. mTORC2 targets AGC kinases through Sin1-dependent recruitment. *Biochem J* 2011;439:287–97.
 46. Samuels Y, Waldman T. Oncogenic mutations of PIK3CA in human cancers. *Curr Top Microbiol Immunol* 2010;347:21–41.
 47. Jain A, Arauz E, Aggarwal V, Ikon N, Chen J, Ha T. Stoichiometry and assembly of mTOR complexes revealed by single-molecule pulldown. *Proc Natl Acad Sci* 2014;111:17833–8.

48. Wullschleger S, Loewith R, Oppliger W, Hall MN. Molecular organization of target of rapamycin complex 2. *J Biol Chem* 2005;280:30697-704.
49. Spagnolo L, Rivera-Calzada A, Pearl LH, Llorca O. Three-dimensional structure of the human DNA-PKcs/Ku70/Ku80 complex assembled on DNA and its implications for DNA DSB repair. *Mol Cell* 2006;22:511-9.
50. Bakkenist CJ, Kastan MB. DNA damage activates ATM through intermolecular autophosphorylation and dimer dissociation. *Nature* 2003;421:499-506.
51. Gao D, Inuzuka H, Tseng A, Chin RY, Tokar A, Wei W. Phosphorylation by Akt1 promotes cytoplasmic localization of Skp2 and impairs APCCdh1-mediated Skp2 destruction. *Nat Cell Biol* 2009;11:397-408.